processes

MDPI

Article

Functionalization of Rice Husk for High Selective Extraction of Germanium

Qunshan Wei [1,*], Wei Zeng [1], Siyi Ding [2,*], Zhemin Shen [3], Xinshan Song [1], Yuhui Wang [1], Charles Nzila [4] and Christopher W. K. Chow [5]

[1] College of Environmental Science and Engineering, Donghua University, Songjiang District, Shanghai 201620, China
[2] Institute of Artificial Intelligence, Donghua University, Shanghai 201620, China
[3] College of Environmental Science and Engineering, Shanghai Jiao Tong University, 800 Dongchuan Road, Shanghai 200240, China
[4] School of Engineering, Moi University, Eldoret 3900-30100, Kenya
[5] Sustainable Infrastructure and Resource Management (SIRM), UniSA STEM, University of South Australia, Mawson Lakes, SA 5095, Australia
* Correspondence: qswei@dhu.edu.cn (Q.W.); dingsiy@dhu.edu.cn (S.D.)

Abstract: It is of strategic significance to extract germanium (Ge) in an ecological way for sustainable development. Adsorbents that already adsorb Ge have disadvantages such as poor selectivity and low adsorption capacity. In this study, a novel adsorbent material based on rice husk functionalized with tannic acid was developed for the efficient extraction of Ge from simulated coal fly ash leachate. The adsorption capacity of tannic acid-functionalized rice husk (TA-EPI-ORH) for Ge was 19.9 times higher than that of untreated rice husk, demonstrating significantly improved performance. The results showed that the adsorption process of Ge by TA-EPI-ORH is consistent with pseudo-second-order kinetic and Freundlich isotherm model. TA-EPI-ORH had excellent selective adsorption properties, with adsorption of 1.40 mg L^{-1} Ge exceeding 95% and solid-liquid partition coefficients of 4380 mL g^{-1}, even in the presence of nine impurity metal ions (average concentration: 479.08 mg L^{-1}). When compared with the two main coexistence ions—aluminum (Al) and calcium (Ca)—both of which have the relatively highest concentrations (Al: 1594.20 mg L^{-1}, Ca: 1740.13 mg L^{-1}), the separation factors for Ge still maintain relatively high level with SF(Ge/Al) = 42.57 and SF(Ge/Ca) = 39.93. Compared to existing studies, TA-EPI-ORH exhibits superior selective adsorption performance even with the presence of more interfering ions. After elution of the adsorbed Ge from TA-EPI-ORH, the extraction rate of Ge with low initial concentration (1.40 mg L^{-1}) reached 85.17%, while the extraction rates of Al and Ca were only 1.02% and 1.18%, respectively. Further research revealed that the catechol groups on the surface of TA-EPI-ORH formed stable complexes with Ge, whereas the complexes with coexisting ions (e.g., Ca and Al) were unstable, thereby ensuring high selectivity for Ge. This green chemistry-based functionalization of rice husk not only enables high-value utilization of agricultural waste but also provides a sustainable and eco-friendly strategy for efficient Ge separation and recovery.

Keywords: germanium; adsorption; rice husk; tannic acid; separation

check for updates

Academic Editor: Juan García Rodríguez

Received: 27 March 2025
Revised: 25 April 2025
Accepted: 25 April 2025
Published: 29 April 2025

Citation: Wei, Q.; Zeng, W.; Ding, S.; Shen, Z.; Song, X.; Wang, Y.; Nzila, C.; Chow, C.W.K. Functionalization of Rice Husk for High Selective Extraction of Germanium. *Processes* **2025**, *13*, 1367. https://doi.org/10.3390/pr13051367

Copyright: © 2025 by the authors. Licensee MDPI, Basel, Switzerland. This article is an open access article distributed under the terms and conditions of the Creative Commons Attribution (CC BY) license (https://creativecommons.org/licenses/by/4.0/).

1. Introduction

Germanium (Ge) is a rare metal, and it plays a significant part in the production of semiconductors [1], optical fiber for communication [2], solar cells as catalysts [3] and optics for infrared systems [2] due to its distinctive electronic and optical properties. The rapid

development of high-technology industries further escalates the demand for Ge. However, Ge has limited natural reserves and does not usually form specific deposits in nature; it is quite often present in various associated minerals [4], which adds complexity to the mining process and limits the stability of its supply. Hence, it is of strategic importance to explore new ways to extract Ge from sources to meet the market demand. The current sources of Ge are mainly concentrated in two secondary sources, lead and zinc smelting slag and coal fly ash [5–7].

Leaching Ge from coal fly ash requires several steps, and in the first step (the pretreatment step), the leachate, which still contains numerous impurity ions (Al, Fe, Ca, Mg), is further separated and purified. Currently, common conventional Ge extraction methods include chemical precipitation [8], solvent extraction [9–12], ion-exchange [13], flotation [14,15], $GeCl_4$ distillation [5], etc. However, these methods suffer from low efficiency, high cost, and potential risk of environmental pollution in the treatment of coal fly ash [16]. Adsorption is considered the optimal method for extracting Ge from acid leachate of coal fly ash due to its high efficiency, low cost, and environmental friendliness [17]. This method efficiently enriches and separates Ge elements through physical or chemical adsorption. Compared with traditional chemical methods, adsorption decreases chemical reagent use, energy consumption, and environmental pollution [18]. Cui et al. [19] synthesized catechol-functionalized nanosilica, which exhibited a maximum Ge adsorption capacity of 5.75 mg g^{-1} at pH 4.5. In contrast, the catechol-formaldehyde resin synthesized by Cruz et al. [20] showed a lower Ge adsorption capacity of 3 mg g^{-1} at pH 6. Although adsorbent materials for Ge adsorption have also been studied, the existing materials have the disadvantages of low adsorption capacity and poor selective adsorption ability [18]. Adsorbent materials with excellent selective adsorption performance are urgently needed for Ge adsorption, especially for the coal fly ash leaching solution where a large number of impurity ions exist.

The structure of tannic acid (TA) is rich in multiple catechol groups, which demonstrates high Ge selectivity in solvent extraction, complexation, ion exchange, and solid phase extraction [18]. TA, a polyphenol sourced from various origins, plays a crucial role in the food industry and environmental applications [8]. Notably, polymeric solids with hydroxyl groups, such as N-methylglucosamine, and polyphenol derivatives, have been used for Ge pre-enrichment and separation [18,20–24]. TA forms precipitate with various metal ions, complicating the precise precipitation of specific ions and potentially leading to co-precipitation of other ions, thereby reducing the purity of the target ion recovery.

Many adsorbent materials have been reported in the literature for the extraction of germanium, such as polyurethane foams [25], activated carbon [26], titanium dioxide nanoparticles [27]. However, these materials have a low affinity for Ge, so the selective adsorption in complex systems is poor [28]. In addition, most materials are more costly and less utilized. Currently, the world is paying more and more attention to environmental issues and seeking green development. Biomass waste is gradually being emphasized, and a lot of it is being used for the treatment of metal ions [29–31]. These studies have shown that biomass waste can be used as a preferred adsorption material for metal ions. This material not only has a high adsorption efficiency but also significantly reduces environmental pollution and provides a sustainable solution for the resourceful utilization of rare metals. As an agricultural waste, the low cost and renewability of rice husk (RH) provide both economic and environmental advantages for Ge extraction [32]. Previously, RH was primarily discarded or used for simple combustion purposes, leading to significant resource waste and potential environmental pollution [33]. As an agricultural byproduct, RH contains a large amount of cellulose, hemicellulose, and lignin, which are easily degradable and biocompatible. However, the adsorption capacity of RH is usually low due to inter-

molecular hydrogen bonding between cellulose hydroxyl groups present in the RH [34]. Notably, chemical modification of biomass materials can improve their adsorption capacity as well as selectivity [35]. The selection of RH as a carrier for TA offers several advantages. Firstly, it is abundantly available and cost-effective, hence suitable for large-scale metal ion treatment. Secondly, being a natural biomass, RH does not cause secondary environmental pollution, making it ideal for water treatment and related applications. It is notable that no studies have been conducted on the modification of RH with TA.

This study presents an innovative approach to valorizing agricultural waste through the development of a sustainable adsorbent material derived from RH functionalized with TA. The adsorbent's performance was systematically evaluated, including its adsorption kinetics, equilibrium isotherm behavior, and selective binding affinity toward Ge. This work not only advances the field of functionalized bio-based adsorbents but also underscores the potential of agricultural byproducts in circular economy strategies for sustainable resource management.

2. Experiment and Method

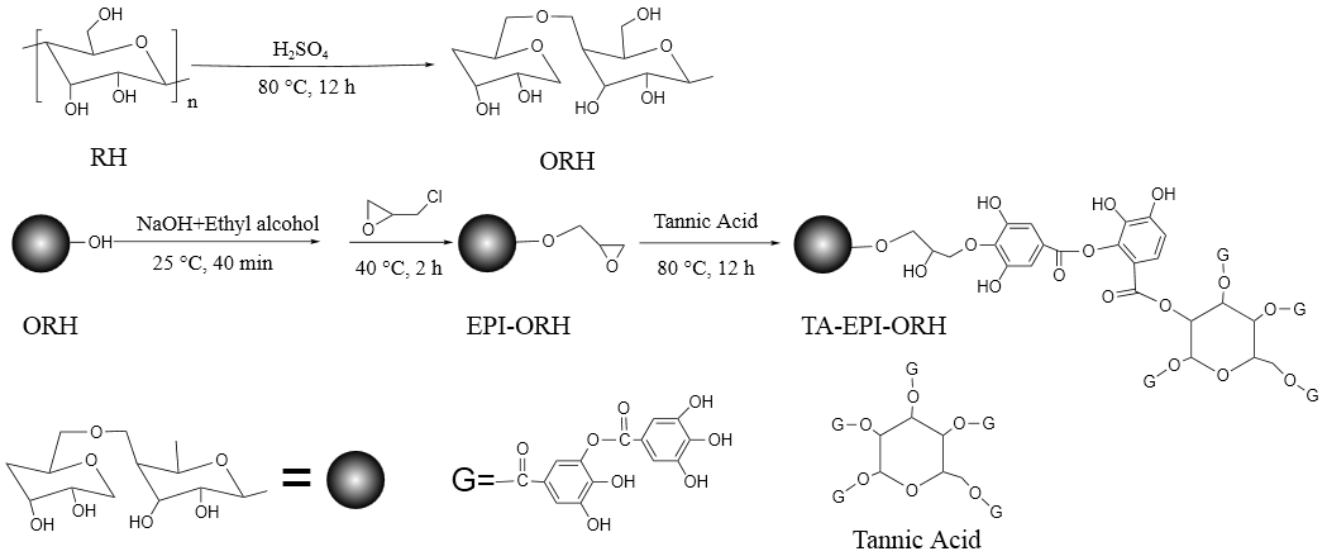
2.1. Materials and Reagents

RH was collected from a farm and crushed to 10 mesh before being used. Gallium nitrate hydrate ($Ga(NO_3)_3 \cdot xH_2O$, 99.9%) was sourced from Shanghai McLean Biochemical Technology Co. TA ($C_{76}H_{52}O_{46}$, 96%), and Ge dioxide (GeO_2, 99.999%) were purchased from Shanghai Yuanye Biotechnology Co. HNO_3 (GR, 65~68%), $AlCl_3 \cdot 6H_2O$ (AR, ≥97%), $FeCl_3$ (CP, ≥97%), KCl (GR, ≥99.8%), NaCl (AR, ≥99.8%), HCl (GR, 36~38%), $ZnCl_2$ (AR, ≥98%), $CuCl_2 \cdot 2H_2O$ (AR, ≥98%), $MgCl_2 \cdot 6H_2O$ (AR, ≥98%), NaOH (AR, ≥99%), and H_2SO_4 (CP, 95~98%) were purchased from Sinopharm Chemical Reagent Co in China. Anhydrous ethanol (C_2H_5OH, ≥99.7%) was purchased from Shanghai Titan Technology Co., Ltd. Epichlorohydrin (C_3H_5ClO, AR, ≥99%) was purchased from Shanghai Bohr Chemical Reagent Co. Sodium bicarbonate ($NaHCO_3$, ≥99.5%) was purchased from Shanghai Haohong Biomedical Technology Co., Ltd. Ge storage solution (1.5 g L^{-1}): dissolved 0.2161 g GeO_2 with 4.1 mL of 1 mol L^{-1} NaOH solution, and then volumed it into a 100 mL volumetric flask. All reagents were used directly without further purification.

2.2. Synthesis of Adsorbents

Step 1: Preparation of carbonized RH

In order to increase the reactivity of hydroxyl groups in RH, the RH was first chemically treated using sulfuric acid. The synthesis of carbonized RH was based on the method reported in previous work [33]. Carbonized RH was prepared from RH by sulfuric acid treatment. 10.00 g crushed RH was placed into a 250 mL three-mouth round bottom flask, and 80 mL 95~98% sulfuric acid was added to it. The mixture was returned in a magnetic stirring water bath at 80 °C for 12 h. After the black suspension was cooled, it was filtered by a circulating water vacuum pump and washed with distilled water and sodium bicarbonate until the filtrate was neutral. The sulfuric acid-treated RH was dried at 50 °C in a drying oven, then grounded and sieved using a 50–100 mesh and abbreviated as ORH. The entire synthesis process from RH to adsorbent (TA-EPI-ORH) can be seen in Scheme 1. Epoxy groups are introduced into the RH by epichlorohydrin, an electrophilic reagent, through its reaction with the primary hydroxyl groups on the sulfuric acid-activated RH [36]. As a highly reactive epoxy group, it reacts with the carboxyl group of TA. This reaction breaks the C-O bond and opens the epoxy ring [37], successfully grafting TA onto the RH.



Scheme 1. The preparation process of TA-EPI-ORH.

Step 2: Preparation of epoxidized RH

A 5.00 g ORH was weighed and transferred into a 250 mL three-mouth round bottom flask, and 80 mL 0.1 g mL^{-1} of NaOH and anhydrous ethanol (volume ratio 1:1) were added. The mixture was stirred at 25 °C for 40 min, then 25 mL epichlorohydrin was added, and the mixture was refluxed in a magnetic stirring water bath at 40 °C for 2 h. The mixture was then filtered by a circulating water vacuum pump and washed with distilled water until the filtrate was neutral. The filtered product was dried at 50 °C using a drying oven and named EPI-ORH.

Step 3: Preparation of TA functionalized RH

A 120 mL 0.15 mol L^{-1} TA solution was added to the three-mouth round bottom flask, and then 2.00 g of the epoxidized RH (EPI-ORH) prepared above was added. The mixture was stirred in a magnetic stirring water bath at 80 °C for 12 h. The mixture was then filtered by a circulating water vacuum pump and washed with distilled water until the filtrate was neutral. The filtered product was dried under a vacuum in a drying oven at 40 °C for 12 h. Then it was grounded and sieved using a 50–325 mesh and used as the adsorbent, target product (TA-EPI-ORH).

2.3. Adsorption Experiment

2.3.1. Effect of pH on Ge Adsorption

A 15 mg L^{-1} Ge solution was prepared by using Ge storage solution, and its pH was adjusted using 1 mol L^{-1} HCl and NaOH to obtain initial pH values of 1.00, 2.00, 3.00, 4.00, and 5.00. Subsequently, 20 mg of TA-EPI-ORH was precisely transferred to a 100 mL conical flask containing 20 mL of the corresponding Ge solution. The mixture was transferred to a water bath shaker at 30 °C and stirred at 150 r/min for 10 h. After adsorption, we utilized a 0.45 μm membrane to filter the mixed solution. The concentration of Ge before and after adsorption was determined by an inductively coupled plasma atomic emission spectrometer (ICP-OES). In this case, the adsorption capacity at equilibrium can be calculated using the following Equations (1) and (2).

$$E = (C_0 - C_e)/C_0 \times 100\% \quad (1)$$

$$Q_e = (C_0 - C_e) \times V/m \quad (2)$$

where E is the adsorption rate, Q_e (mg g^{-1}) is the equilibrium adsorption capacity of the adsorbent, C_0 and C_e are the Ge ion concentration in the initial and equilibrium state of the aqueous solution (mg L^{-1}), respectively, V is the volume of the initial Ge solution (L), and m is the mass of the added TA-EPI-ORH adsorbent (g).

2.3.2. Effect of Adsorbent Mass on Ge Adsorption

Respective weights of 10, 20, 30, 40, and 50 mg of TA-EPI-ORH were put into 100 mL conical flasks. A 15 mg L^{-1} Ge solution was prepared by using Ge storage solution and adjusted to pH 2 using 1 mol L^{-1} HCl and NaOH. Added 20 mL Ge solution to each 100 mL conical flask filled with adsorbent. The mixture was placed in a 30 °C water bath shaker and agitated at 150 r/min for 10 h. After adsorption, the Ge concentration before and after adsorption was measured using the method described in Section 2.3.1.

2.3.3. Effect of Adsorbent Type on Ge Adsorption

A 15 mg L^{-1} Ge solution was prepared by using Ge storage solution and adjusted to pH 2 using 1 mol L^{-1} HCl and NaOH. Then, 20 mg of each adsorbent (RH, ORH, EPI-ORH, and TA-EPI-ORH) was weighed into separate 100 mL conical flasks, and 20 mL of the Ge solution (pH 2) was added to each. The mixture was placed in a 30 °C water bath shaker and agitated at 150 r/min for 10 h. After adsorption, the Ge concentration before and after adsorption was measured using the method described in Section 2.3.1.

2.3.4. Effect of Time on Ge Adsorption

A 15 mg L^{-1} Ge solution was formulated from Ge storage solution and adjusted to pH 3 using 1 mol L^{-1} HCl and NaOH. Subsequently, 20 mL of this solution was added to nine 100 mL conical flasks, each containing 40 mg of TA-EPI-ORH. The mixture was shaken in a water bath at 150 r/min, 25 °C for 15 min, 30 min, 1 h, 2 h, 4 h, 6 h, 8 h, 12 h and 24 h, respectively. After adsorption, the Ge concentration before and after adsorption was measured using the method described in Section 2.3.1.

2.3.5. Adsorption Isotherm

Ge storage solution was used to prepare 20 mL of Ge solutions with concentrations ranging from 10 to 80 mg L^{-1} in 100 mL conical flasks. Adjusted the pH of these solutions to 3 utilizing 1 mol L^{-1} HCl and NaOH and added 40 mg of TA-EPI-ORH adsorbent to each flask. The mixture was put into a water bath shaker and agitated at 150 r/min for 12 h at temperatures of 25 °C, 35 °C, 45 °C and 55 °C. After adsorption, the Ge concentration before and after adsorption was measured using the method described in Section 2.3.1.

2.3.6. Selective Adsorption Study

In actual environments, Ge often coexists with various ions, particularly in coal fly ash acid leachates, which contain significant concentrations of other metal ions (Al, Fe, Ca, Mg). Therefore, it is crucial to investigate the selective adsorption capabilities of adsorbent materials. To study selective adsorption, we formulated a simulated solution based on the metal ions present in coal fly ash acid leachates, using compounds of these metals. The specific composition of the simulated solution is detailed in Table 1. The pH of the simulated solution was adjusted to pH 2 using 1 mol L^{-1} HCl and NaOH, 20 mL of the simulated solution was taken in a 100 mL conical flask, and 60 mg of TA-EPI-ORH adsorbent was added to it. The mixture was put into a water bath shaker and agitated at 150 r/min for 12 h at 25 °C. After adsorption, an appropriate amount of the solution was taken with a syringe and filtered by using a 0.45 μm membrane. The concentrations of Ge and coexisting ions before and after adsorption were measured by ICP-OES. The solid-liquid distribution (partitioning) coefficient (K_d) is the ratio of the adsorbed amount

to the amount remaining in solution [18], which can be calculated by Equation (3), and the separation factor (SF) of Ge with respect to other metal ions in competitive adsorption experiments can be calculated by Equation (4).

$$K_d = (C_0 - C_e)/C_e \times V/m = Q_e/C_e \quad (3)$$

$$SF(Ge/M) = K_{d(Ge)}/K_{d(M)} \quad (4)$$

where Q_e (mg g^{-1}) is the equilibrium adsorption capacity of the adsorbent, C_0 and C_e are the Ge ion concentration in the initial and equilibrium state of the aqueous solution (mg L^{-1}), respectively, V is the volume of the initial Ge solution (L), and m is the mass of the added TA-EPI-ORH adsorbent (g). K_d (L g^{-1}) is the solid-liquid distribution (partitioning) coefficient. $K_{d(Ge)}$ and $K_{d(M)}$ are the partition coefficients of Ge and other metal ions in solution. SF is the separation factor.

Table 1. Composition of metal ions in selective adsorbed solution (units: mg L^{-1}).

Initial Ge	Competing Ion								
	Al	Fe	Ca	Zn	Cu	Mg	Na	K	Ga
14.63	1575.90	249.07	1740.13	4.53	1.93	523.80	191.10	120.27	12.00
1.40	1594.20	236.33	1740.13	4.13	1.87	515.80	98.73	119.60	0.97

2.4. Desorption

Desorption of adsorbent plays an essential role in evaluating the commercial and practical feasibility of the extraction process. In this study, an acidic solution (hydrochloric acid, nitric acid, sulfuric acid) and distilled water were selected for the desorption of Ge from the adsorbent. TA-EPI-ORH loaded with Ge was added to 25 mL eluent and shaken for 12 h at 25 °C and 150 r/min on a water bath shaker. After shaking equilibrium, the solution was filtered by using a 0.45 μm membrane, and the Ge concentration in the filtrate was determined by ICP-OES. Elution experiments were conducted after adsorption in simulated solutions using 1, 2, and 3 mol L^{-1} HNO_3 as eluents. Adsorption experiments were performed according to the procedure in Section 2.3.6. After adsorption, the solution was filtered, and the adsorbent was transferred to a conical flask containing 20 mL of HNO_3 solution (1, 2, or 3 mol L^{-1}). The mixture was put into a water bath shaker and eluted at 150 r/min for 12 h at 25 °C. After elution, the solution was taken with a syringe and filtered by using a 0.45 μm membrane, and the concentrations of Ge and coexisting metal ions before and after adsorption were measured by ICP-OES.

2.5. Analytical Method

Filtration was carried out by a circulating water vacuum pump (SHZ-D). The unfunctionalized RH and the functionalized adsorbent TA-EPI-ORH were characterized by Fourier transform infrared spectroscopy (FTIR, Nicolet6700, United States of America). The FTIR scanning range was from 400 to 4000 cm^{-1}. The adsorbent surface area and pore size were measured by a fully automated rapid, specific surface and porosity analyzer (Autosorb-iQ, Quantachrome Instruments U.S., Beijing, China). Electron micrographs of the adsorbents were obtained using a scanning electron microscope (SEM, Quanta 250, The Czech Republic, FEI, Czech Republic). The elemental composition of the adsorbent and the adsorbent after loading with Ge (TA-EPI-ORH-Ge) were measured by X-ray photoelectron spectroscopy (XPS, Escalab 250Xi, Thermo Fisher, USA). The concentrations of Ge and coexisting metal ions in the test solutions and leachates were measured by inductively coupled plasma atomic emission spectrometer (Agilent 5100/5110 VDV ICP-OES, Thermo

Fisher, USA). ICP-OES test conditions: RF Power: 1.20 KW, Plsama flow: 12.0 L/min, Replicate read time: 5 s, Replicates: 3. All experiments were carried out more than three times to take the average value

3. Results and Discussion

3.1. Adsorbent Characterization

3.1.1. SEM

SEM images of ORH and TA-EPI-ORH are shown in Figure 1. The two samples had significantly different surface morphologies. As shown in Figure 1a, the particles of ORH are lumpy and more concentrated. After the introduction of TA on the ORH (Figure 1b), the size of the particles became more uniform, and the surface of the particles became more dispersed while comparing the TA-EPI-ORH (Figure 1d,f)) with the ORH (Figure 1c,e), the particles showed a porous structure with the introduction of TA, which means that TA was successfully introduced to the surface of the carbonized rice husk, and at the same time, the TA introduction provides more adsorption space and adsorption sites for Ge adsorption.

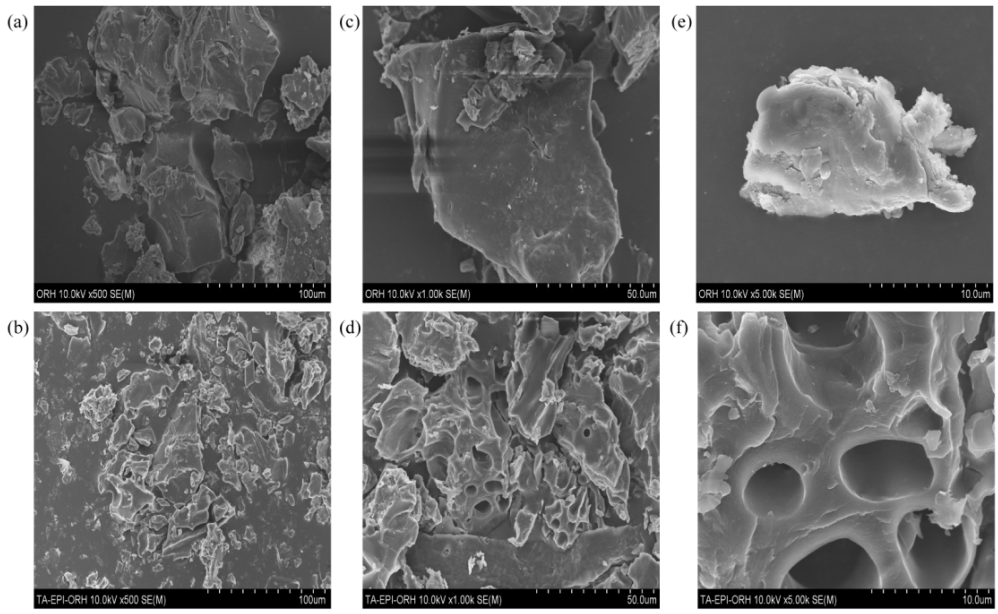


Figure 1. SEM of ORH and TA-EPI-ORH, where (**a**) 500× magnification, (**c**) 1000× magnification, (**e**) 5000× magnification for ORH; (**b**) 500× magnification, (**d**) 1000× magnification, (**f**) 5000× magnification for TA-EPI-ORH.

3.1.2. FTIR

Figure 2a shows the FTIR spectra of ORH, EPI-ORH, TA-EPI-ORH, and TA-EPI-ORH-Ge. In the ORH spectrum, the peak at 3432 cm^{-1} comes from the -O-H stretching vibration [33,38], and the four materials, ORH, EPI-ORH, TA-EPI-ORH, and TA-EPI-ORH-Ge, all contain hydroxyl functional groups, whether modified or not. The peak at 2939 cm^{-1} corresponds to the stretching vibration of the -CH bond, while the peak at 1211 cm^{-1} is identified as the stretching vibration of C-O-C [33,39]. After the ring-opening reaction with TA, a new peak at 1712 cm^{-1} was found, which corresponded to the C = O of TA [37], in addition to the spectral bands between 1321 and 1612 cm^{-1}, which corresponded to the benzene ring skeleton vibration [8,37], and the peak observed at 1035 cm^{-1} is consistent with the stretching vibration of the C-O bond [33], which indicated that TA-EPI-ORH was successfully synthesized.

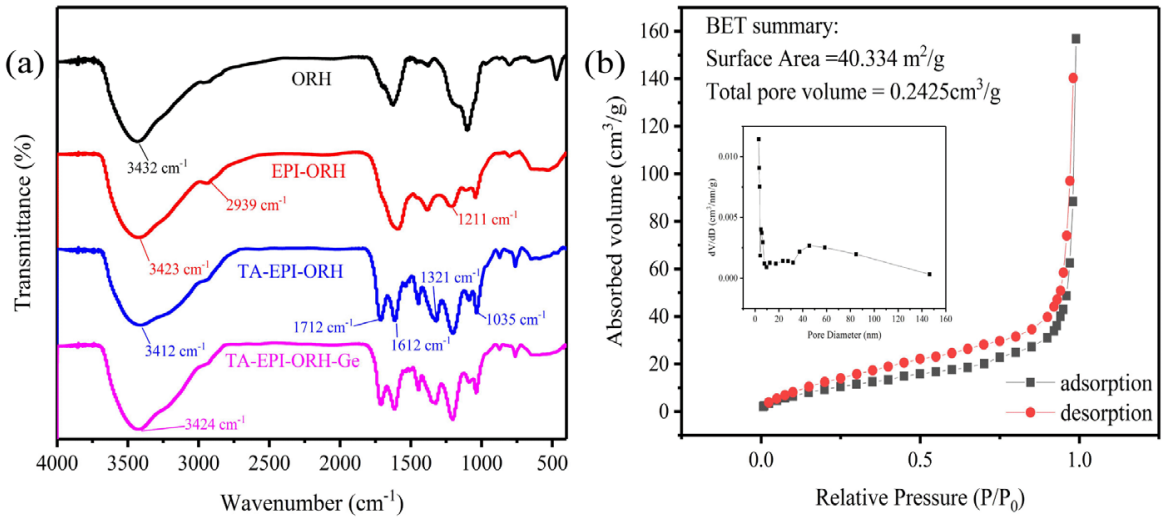


Figure 2. (**a**) FTIR spectra of ORH, EPI-ORH, TA-EPI-ORH, and TA-EPI-ORH-Ge; (**b**) nitrogen adsorption and desorption curves of TA-EPI-ORH.

3.1.3. Specific Surface and Porosity Analyser

The nitrogen adsorption and desorption curves, as well as the pore size distribution of TA-EPI-ORH are given in Figure 2b. The results showed that the specific surface area of TA-EPI-ORH was 40.334 m^2 g^{-1}, and the total pore volume was 0.2425 cm^3 g^{-1}. According to the definition of the International Union of Pure and Applied Chemistry (IUPAC), there existed mesopores (2~50 nm) in TA-EPI-ORH, and the material had a large amount of specific surface area and pore structure, which are conducive to the Ge adsorption.

3.2. Effect of pH on Ge Adsorption

The pH value of the solution is a critical factor that influences the adsorption process; it not only just affects the chemical properties and surface properties of the adsorbent but also affects the morphology of Ge ions in the solution. The morphological distribution of Ge ions varies under different pH conditions. In aqueous solution, Ge is found in three main forms: $Ge(OH)_4$, the anion $GeO(OH)_3^-$ and $GeO_2(OH)_2^{2-}$ [20,40]. In the range of pH 1~9, Ge mainly exists in the form of $Ge(OH)_4$; at pH 9~12.5, Ge mainly exists in the form of $GeO(OH)_3^-$, and at pH above 12.5, Ge mainly exists in the form of $GeO_2(OH)_2^{2-}$ [40]. Since the application of adsorbent was to adsorb Ge in an acidic solution, this study explored the effect of pH on the adsorbent's adsorption of Ge in an acidic environment, and the results are shown in Figure 3a. TA-EPI-ORH adsorption experiments on Ge were carried out in the range of pH 1~5. As the pH level rose from 1 to 5, the adsorption capacity of Ge increased significantly. This is because the concentration of hydrogen ions in the solution decreased with the increase in pH. As the pH increased, the competition between Ge ions and hydrogen ions was weakened, which resulted in an increase in Ge adsorption capacity. The morphological distribution of metal ions in the leach solution was calculated using Visual MINTEQ 3.1 (Visual MINTEQ, ver. 3.1.), and Figure 3d,e show the morphological distribution of different metal ions with pH, and the results show that iron ions may precipitate when the pH is greater than 3. Meanwhile, to better investigate the competitive adsorption of Ge in acidic solutions, the pH was selected to be below 3 in order to assess the adsorption performance of TA-EPI-ORH on Ge.

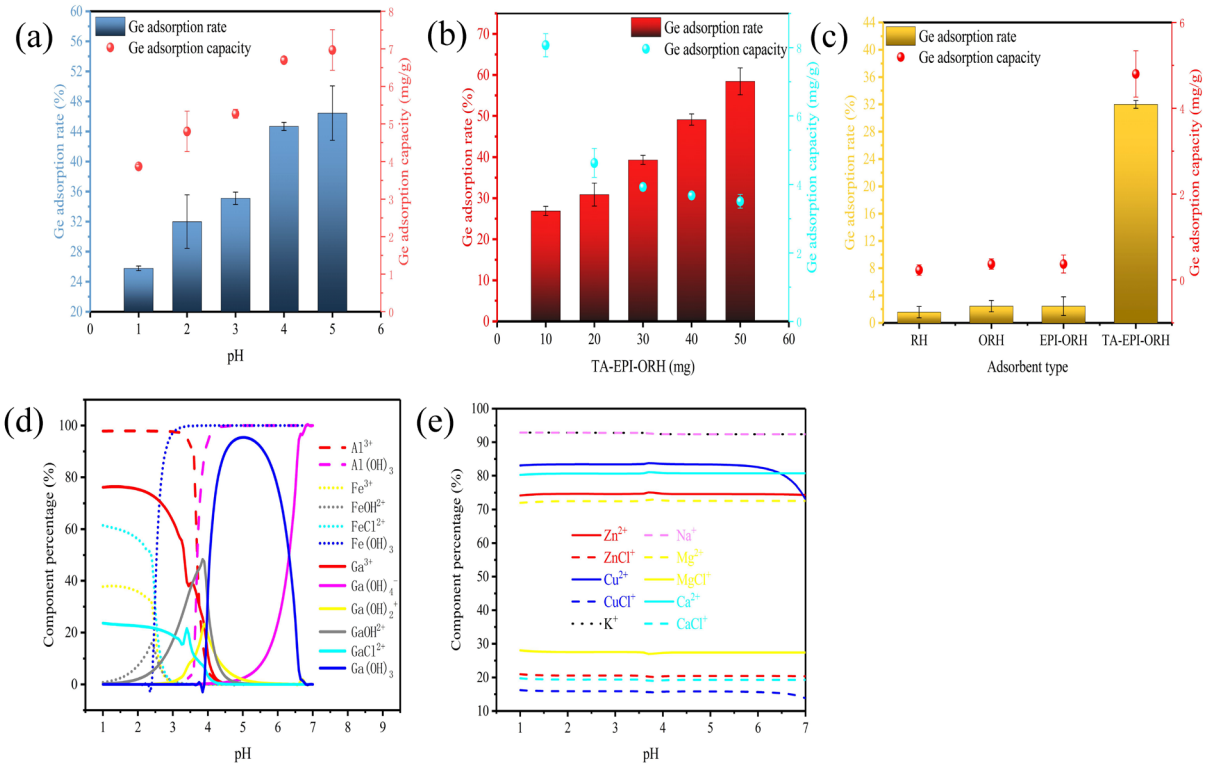


Figure 3. Effect of factors (**a**) pH, (**b**) amount of adsorbent, (**c**) adsorbent type on Ge adsorption and morphological distribution of metal ions with pH change (**d**,**e**).

3.3. Effect of Adsorbent Mass on Ge Adsorption

In this study, the effect of adsorbent mass on Ge adsorption was analyzed, and the results are shown in Figure 3b. The adsorption rate of Ge increased with the increase of adsorbent mass, but the adsorption capacity gradually decreased. This may be because of the fact that the active sites available for Ge adsorption increased with the increase of adsorbent mass, and the adsorption rate increased, but at the same time, the concentration of Ge in the solution became the main limiting factor of the adsorption capacity, and thus the adsorption capacity gradually decreased.

3.4. Effect of Adsorbent Type on Ge Adsorption

In this study, the adsorption effects of different kinds of adsorbents on Ge were also compared, and the results are shown in Figure 3c. The results showed that the adsorption efficiency of TA-modified RH was higher than untreated RH. The adsorption capacity of untreated RH for Ge was only 0.23 mg g^{-1} after 10 h at a solid-liquid ratio of 20 mg:20 mL, pH 2, 150 r/min, and 30 °C, whereas TA-EPI-ORH achieved an adsorption capacity of 4.80 mg g^{-1} under the same conditions. FTIR analysis suggests that this improvement is likely due to the introduction of TA during modification, which enhances interactions and improves adsorption performance. In addition, the adsorption effect of TA-EPI-ORH on Ge in an acidic solution is higher than that of EPI-ORH, mainly because the TA structure contains many catechol groups, which show good complexation on Ge. Therefore, compared with epoxidized RH, TA functionalized RH has a significant adsorption capacity for Ge, and the introduction of TA enhances the surface activity of RH, thereby improving the adsorption capacity of Ge. From the SEM and FTIR analyses, the introduction of TA into RH increased the adsorption space and active sites on the surface of RH, which could improve the adsorption capacity of Ge.

3.5. Effect of Adsorption Time on Ge Adsorption

Adsorption kinetics is an important factor to explore the adsorption mechanism; in this study, the results of Ge adsorption by TA-EPI-ORH were analyzed by using the pseudo-first-order kinetic model and the pseudo-second-order kinetic model. For the adsorption process of Ge, the kinetic model can be expressed as follows [38]:

$$Q_t = Q_{em}(1 - \exp^{-k1t}) \quad (5)$$

$$t/Q_t = 1/(k_2 Q_{em}{}^2) + t/Q_{em} \quad (6)$$

where Q_{em} (mg g^{-1}) and Q_t (mg g^{-1}) are the amount of Ge adsorbed by TA-EPI-ORH at equilibrium and time t (h), respectively, and k_1 (h^{-1}), k_2 ($g \cdot mg^{-1} \cdot h^{-1}$) are the adsorption rate constants for the pseudo-first-order and pseudo-second-order kinetic model, respectively.

Figure 4a depicts the results of adsorption kinetics. At an initial Ge concentration of 15 mg L^{-1}, the Ge adsorption reached equilibrium at about 8 h. In addition, the specific parameters of adsorption kinetics are listed in Table 2. The results showed that R^2 (R^2 = 0.94) of the pseudo-second-order kinetic model was greater than that of the pseudo-first-order kinetic model (R^2 = 0.79), and the equilibrium adsorption capacity of the pseudo-second-order kinetic model (3.61 mg g^{-1}) was closer to the experimental equilibrium adsorption capacity (3.77 mg g^{-1}) than that of the pseudo-first-order kinetic model (3.38 mg g^{-1}). Therefore, it shows that the pseudo-second-order kinetic model provides a superior match to experimental data. It shows that the adsorption process of Ge by TA-EPI-ORH was mainly controlled by chemical adsorption [17]. From the FTIR analysis, the hydroxyl group in TA-EPI-ORH interacted with Ge, which can be further verified [37].

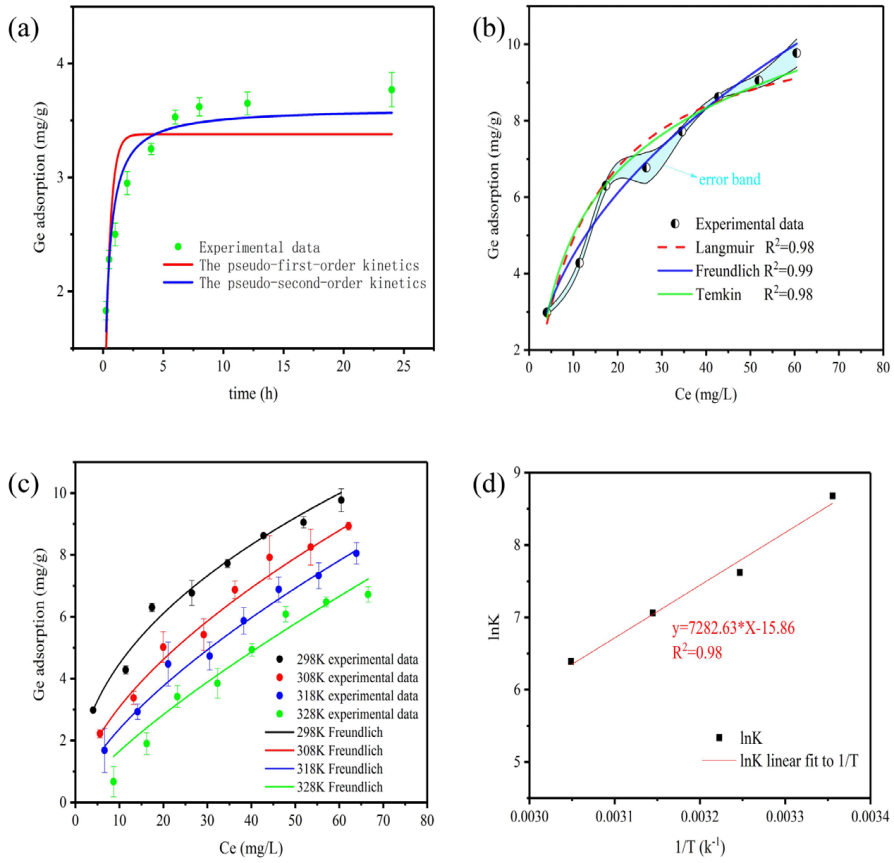


Figure 4. Adsorption kinetics (**a**), adsorption isotherms (**b**,**c**), and Van't Hoff equation (**d**) for Ge adsorption by adsorbent.

Table 2. Kinetic parameters of Ge adsorption by TA-EPI-ORH.

Pseudo-First-Order				Pseudo-Second-Order		
Experimental Equilibrium Q_e (mg g^{-1})	**Model Equilibrium Q_{em} (mg g^{-1})**	**k_1 (h^{-1})**	**R^2**	**Model Equilibrium Q_{em} (mg g^{-1})**	**k_2 (g mg^{-1} h^{-1})**	**R^2**
3.77	3.38	2.34	0.79	3.61	0.93	0.94

3.6. Adsorption Isotherm

Adsorption isotherms can be used to evaluate the maximum adsorption capacity of adsorbents and are widely used in studies to understand adsorption mechanisms. In this study, three adsorption isotherm models were used to fit the experimental data, and the expressions of the three adsorption isotherm models are as follows:

$$\text{Langmuir} : Q_e = \frac{Q_{max} \times K_L \times C_e}{1 + K_L \times C_e} \quad (7)$$

$$\text{Freundlich} : Q_e = K_F \times {C_e}^{1/n} \quad (8)$$

$$\text{Temkin} : Q_e = R \times T/b \times \ln(A \times C_e) \quad (9)$$

where Q_e (mg g^{-1}) is the equilibrium adsorption capacity of TA-EPI-ORH for Ge, C_e (mg L^{-1}) is the residual concentration of Ge in the solution after adsorption equilibrium, Q_{max} is the theoretical saturated adsorption capacity (mg g^{-1}), K_L (L mg^{-1}) is the Langmuir equilibrium constant, K_F ((mg g^{-1})·(L mg^{-1})$^{1/n}$) is the Freundlich isotherm constant, n is the adsorption strength, R is the gas constant of 8.314 J mol^{-1} K^{-1}, T is the kelvin temperature (K), b is the Temkin constant, and A (L mg^{-1}) is the Temkin isotherm constant.

Figure 4b,c show the influence of Ge concentration on the adsorption capacity of TA-EPI-ORH on Ge at different temperatures (25 °C, 35 °C, 45 °C, 55 °C). The corresponding parameters fitted by Langmuir, Freundlich, and Temkin isotherm models were calculated and summarized in Table 3. From the linear correlation coefficient, the adsorption isotherm of Ge on TA-EPI-ORH was consistent with the Freundlich model (R^2 = 0.99), indicating that it is a multilayer adsorption on TA-EPI-ORH. It is worth noting that for the Freundlich isotherm model, n > 1 indicates that the adsorbent can be easily adsorbed on the adsorbent [37]. In this study, the value of n in the Freundlich model is 2.24 (>1), indicating that Ge can be easily adsorbed by TA-EPI-ORH adsorbent.

Table 3. Parameters associated with the TA-EPI-ORH adsorption isotherm of Ge (25 °C; pH = 3).

Isotherm Model	Parameters	TA-EPI-ORH
Langmuir	Q_{max} (mg g^{-1})	10.98
	k_L (L mg^{-1})	0.081
	R^2	0.98
Freundlich	n	2.24
	k_F ((mg g^{-1})·(L mg^{-1})$^{1/n}$)	1.60
	R^2	0.99
Temkin	A (L mg^{-1})	0.82
	b ((kJ mol^{-1})·(g mg^{-1}))	1.04
	R^2	0.98

3.7. Adsorption Thermodynamics

Adsorption thermodynamics focuses on the energy changes of the adsorption process, including the spontaneous, absorptive, or exothermic nature of adsorption [41]. The

interaction of TA-EPI-ORH with Ge can be accounted for by the standard Gibbs free energy change (ΔG^0, kJ mol^{-1}), standard enthalpy change (ΔH^0, kJ mol^{-1}), and standard entropy change (ΔS^0, J mol^{-1} K^{-1}). The parameters of these three can be determined by the following equations [42].

$$K = K_m \times 10^3 \times M_W \times C_{adsorbate}/\gamma_{adsorbate} \quad (10)$$

$$\Delta G^0 = -RTlnK \quad (11)$$

$$\Delta G^0 = \Delta H^0 - \Delta S^0 T \quad (12)$$

$$lnK = \Delta S^0/R - \Delta H^0/RT \quad (13)$$

where K is the adsorption equilibrium constant at different temperatures, K_m is the equilibrium constant to which the adsorption isotherm model is applied and is obtained as Q_e (mg g^{-1}) vs. C_e (mg L^{-1}), $C_{adsorbate}$ is the standard concentration of Ge and is taken as 1 mol L^{-1}, $\gamma_{adsorbate}$ is the activity coefficient of Ge (dimensionless) and is taken as 1, M_w is the molar mass of Ge, which is taken as 72.64 g mol^{-1}, R is the gas constant (8.314 J mol^{-1} K^{-1}), T is the temperature (K), and the values of ΔS° and ΔH° could be calculated by plotting lnK versus 1/T by the intercept and slope, respectively.

The curve of lnK versus 1/T is plotted in Figure 4d, and the thermodynamic-specific parameters are summarized in Table 4. The adsorption of Ge decreases with increasing temperature, and the negative value of ΔH^0 indicates that the reaction is an exothermic process, while ΔG^0 is less than 0, which suggests that the reaction can proceed spontaneously. The value of ΔG^0 gradually becomes smaller with increasing temperature, indicating that increasing temperature is unfavorable for the adsorption conditions.

Table 4. Thermodynamic parameters of Ge adsorption by TA-EPI-ORH.

T(K)	ΔG^0 (kJ mol^{-1})	ΔH^0 (kJ mol^{-1})	ΔS^0 (KJ mol^{-1} K^{-1})
298	−21.51	−60.55	−0.13
308	−19.51		
318	−18.66		
328	−17.42		

3.8. Selective Adsorption Properties

The main objective of this section of the study is to assess the feasibility and selective adsorption of Ge from complex solutions containing multiple coexisting ions. For this purpose, ion adsorption experiments in simulated solutions were performed. The selective adsorption of germanium by TA-EPI-ORH at different initial concentrations of Ge was also investigated in this study, and the specific composition is shown in Table 1. All selective adsorption experiments were performed at pH 2 to avoid precipitation of competing ions. The results of selective adsorption are shown in Figure 5. The results showed that the removal efficiency of TA-EPI-ORH for Ge was much higher (greater than 90%) than that of other competing ions (less than 30%). In addition, the selective adsorption of Ge could be explained by the solid-liquid distribution (partitioning) coefficient (K_d). K_d is the ratio of the adsorption amount to the remaining amount in the solution [18], and the higher the value, the more metal ions adsorbed on the adsorbent and the less metal ions remained in the solution. As demonstrated in Figure 5b, The K_d values of TA-EPI-ORH for Ge were the highest (4.38 and 6.22 L g^{-1}) and several orders of magnitude higher compared to the coexisting ions. At the same time, the separation factor was used to illustrate the separation difficulty of Ge and coexisting ions. If the separation factor is greater than 1, it indicates that the substance can be separated from this substance. As illustrated in

Figure 5c, the separation factors of Ge were much higher than 1 compared with coexisting ions (minimum: SF(Ge/Cu) = 33.18, maximum: SF(Ge/Na) = 174.07), indicating that Ge can be separated from coexisting ions. Table 5 also compares the initial Ge concentration and selectivity of TA-EPI-ORH to some of the adsorbents in the literature. TA-EPI-ORH is more suitable for adsorbing Ge at low concentrations (1.40 mg L^{-1}) in competitive adsorption experiments. This study investigated competitive adsorption experiments that closely mimic the composition of coal fly ash acid leachate, particularly for Al and Ca ions present at concentrations up to thousands of mg L^{-1}. TA-EPI-ORH can overcome the interference of a large number of impurity ions and adsorb low concentrations of Ge efficiently and selectively. The K_d and SF values showed that TA-EPI-ORH exhibited excellent selectivity for Ge in simulated leachate and was more suitable for practical application.

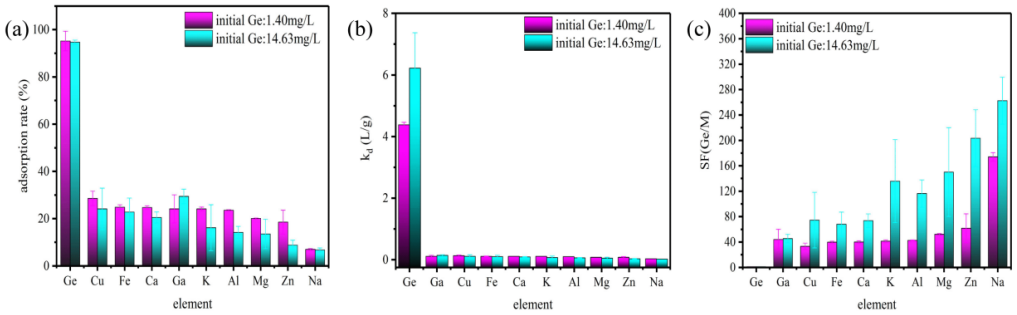


Figure 5. (**a**) adsorption rate, (**b**) K_d, and (**c**) SF of TA-EPI-ORH adsorption of simulated solution.

Table 5. Selectivity comparison of TA-EPI-ORH with other adsorbents.

Absorbent	Selective Results			Refs.
	Composition of Ions (mg L^{-1})	Number of Ions [b]	Ge SF Range [a]	
catechol-functionalized silica	Ge: 10 B: 10, Te: 10 (pH 4.5)	2	5.3 (Te)-281.8 (B)	[19]
catechol-formaldehyde resin	Ge: 10 Zn: 10, Si: 10 (pH 6)	2	5 (Zn)-28 (Si)	[20]
Three Dimension-α-FeOOH	Ge: 5 Ga: 5 (pH 12)	1	Ga (41.56)	[28]
SOL-KELEX	Ge: 51.3 Zn: 2.5, Sb: 4.5, As: 61.8, Ni: 27.8 (pH 6.2)	4	28.7 (Zn)-no ads (Sb)	[43]
TA-EPI-ORH	Ge: 1.40 Al, Ca, Fe, Na, K, Ga, Zn, Cu, Mg (Table 1) (pH 2)	9	33.18 (Cu)-147.07 (Na)	this work

[a]: the range is from lowest SF (ion) to highest SF (ion); [b]: number of competing ions species; no ads: no detected adsorption of the ion.

3.9. Selective Adsorption Mechanism

The XPS spectra of TA-EPI-ORH and TA-EPI-ORH-Ge are shown in Figure 6. The presence of Ge 3d peak in TA-EPI-ORH-Ge indicates that Ge was successfully adsorbed onto the surface of TA-EPI-ORH (Figure 6). The ability of this adsorbent to adsorb Ge with high selectivity is mainly attributed to the introduction of TA, which contains multiple catechol groups. The FTIR analysis shows that the position of a hydroxyl group in TA-EPI-ORH-Ge is from 3412 cm^{-1} to 3424 cm^{-1} compared to TA-EPI-ORH, indicating that hydroxyl group is involved in the reaction [37]. Ge is predominantly present in the form of $Ge(OH)_4$ within the acidic environment. The chelation of the catechol hydroxyl group and $Ge(OH)_4$ in TA-EPI-ORH have a significant impact on the adsorption process. The

catechol groups can be complex with metal ions, and the stability of the complex is usually related to the affinity of the metal ion for the -OH group. In general, the affinity usually increases with increasing charge and coordination number [18]. Because of the higher charge of Ge(IV) and the fact that Ge(IV) could form a six-coordination structure complex with catechol [8,18,20], catechol has a high affinity for Ge, and therefore, TA-EPI-ORH has a high adsorption capacity for Ge. The adsorbent's weak affinity for coexisting ions is attributed to the linear free energy relationship (LFER) between catechol ligands and transition metal ions in aqueous solutions. The [log $K_1(OH^-) < 3$] of the catechol ligand with the alkali metals (Na^+, K^+, Ca^{2+}, and Mg^{2+}) suggests that the complexes formed by catechol with these metal ions are unstable [44]. Despite Al^{3+} having a higher stability constant, [log $K_1(OH^-)$] value of 9.1, its $2s^2$, $2p^1$ electron configuration makes inner-sphere complex formation with catechol less probable [44].

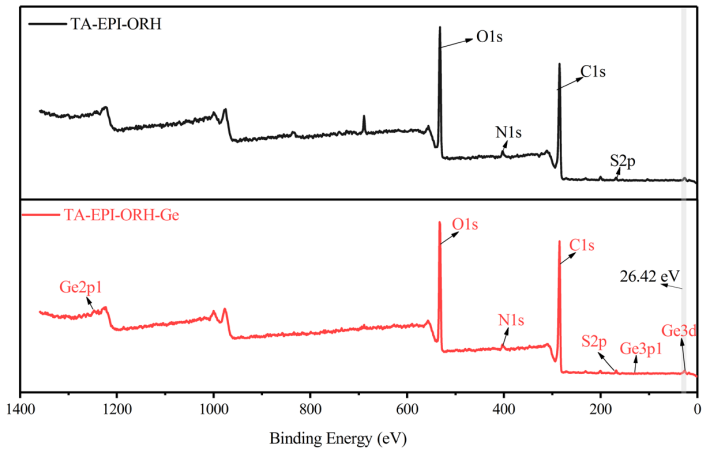


Figure 6. XPS full spectrum scanning of Ge before and after adsorption by TA-EPI-ORH (Ge 3d: 26.42 eV).

3.10. Desorption of Adsorbents

In this study, acidic solutions (hydrochloric acid, nitric acid, sulfuric acid) and distilled water were used for the desorption of Ge from the adsorbent TA-EPI-ORH, with results depicted in Figure 7a. The desorption rate of 1 mol L^{-1} nitric acid outperformed that of 1 mol L^{-1} sulfuric acid and various concentrations of hydrochloric acid. Therefore, after the adsorption of Ge by TA-EPI-ORH, nitric acid can be chosen as the desorption solution for eluting Ge.

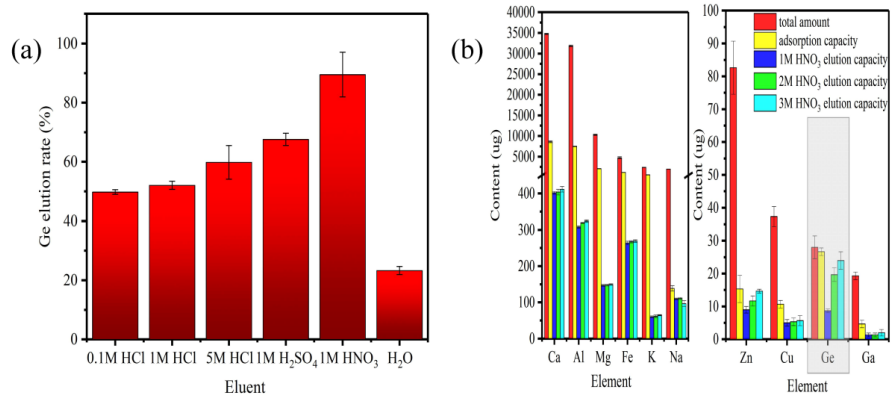


Figure 7. (**a**) Desorption of TA-EPI-ORH loaded Ge by different desorption solutions (M = mol L^{-1}); (**b**) elution amount after adsorption of simulated solutions of TA-EPI-ORH by different concentrations of nitric acid (data in the graphs are absolute contents, total amount: initial absolute content of metal ions during adsorption (μg)).

Using nitric acid as a desorption solution, TA-EPI-ORH adsorbed Ge in the simulated leaching solution was studied. The results in Figure 7b show that nitric acid effectively elutes Ge and exhibits lower elution efficiency for coexisting ions than for Ge. This suggests its potential for further separation of Ge from these ions. In the simulated solution, after TA-EPI-ORH adsorption, Ge elution reached 90% at 3 mol L^{-1} nitric acid, 150 r/min, 25 °C over 12 h. Elution rates of coexisting ions were lower than that of Ge (Al: 4.31%, Ca: 4.78%). Following the adsorption-elution treatment, the Ge extraction rate reached 85.71%, while the extraction rates of coexisting ions were all below 20%, particularly for the abundant impurity ions Al and Ca in the solution, which were only 1.02% and 1.18%, respectively. This demonstrates the efficient and selective Ge extraction capability of TA-EPI-ORH.

3.11. Adsorption Mechanism

The previous adsorption experiments, XPS, and other analyses indicate that TA-EPI-ORH successfully adsorbed Ge. Under the studied conditions, Ge was in the form of $Ge(OH)_4$. In addition, the adsorption kinetics, FTIR, and other analyses indicate that the process of Ge adsorption by TA-EPI-ORH involves chemical adsorption. Specifically, it is the hydroxyl group on TA-EPI-ORH that interacts with Ge [37], so it is hypothesized that the mechanism of Ge adsorption by TA-EPI-ORH may be as shown in Figure 8. The catechol in TA-EPI-ORH forms a complex with Ge [8,18,20], thereby adsorbing the Ge in the adsorbent. In addition, the stability of the complex ensures efficient separation and recovery of Ge [8,18,20,44].

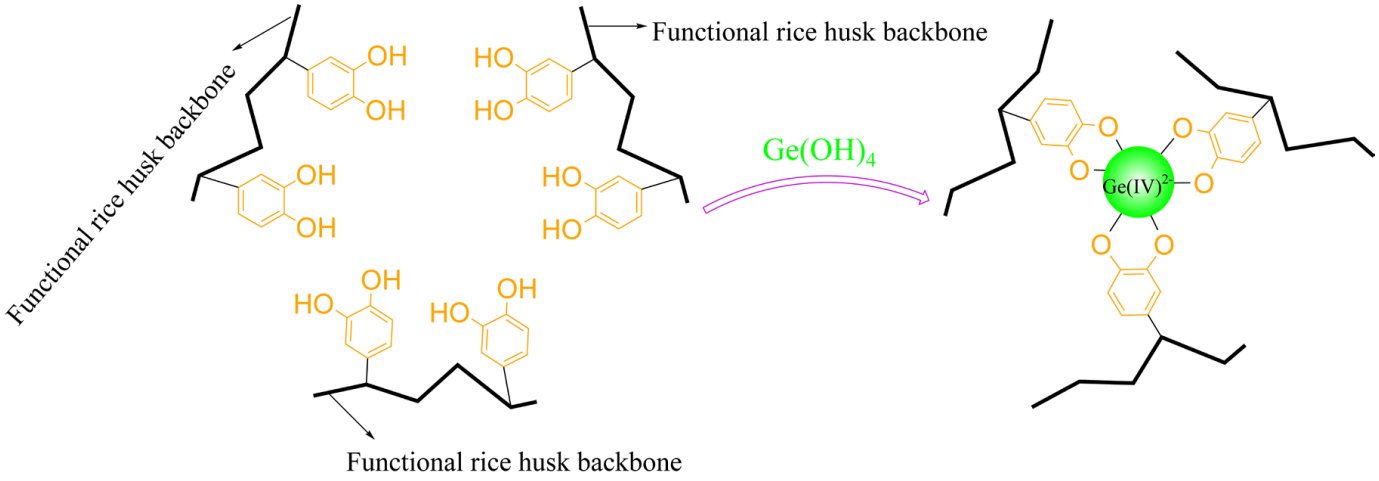


Figure 8. Possible mechanism diagram of Ge adsorption by TA-EPI-ORH.

4. Conclusions

A novel adsorbent, TA-EPI-ORH, was synthesized from RH via a green chemistry approach. The adsorbent was based on the functionalization of TA and had excellent Ge adsorption properties. Compared with untreated RH, the adsorption capacity of TA-EPI-ORH for Ge was increased by 19.9 times, and TA-EPI-ORH reached a maximum of 10.98 mg g^{-1} (pH 3, 25 °C). The Ge adsorption on TA-EPI-ORH followed the Freundlich isotherm and pseudo-second-order kinetic models. TA-EPI-ORH also exhibited an excellent selective adsorption property for Ge in a coal fly ash simulated leachate with nine coexistence ions, of which the average concentration is 479.08 mg L^{-1}. The selective adsorption rate for Ge can reach 95.24% even at a low Ge initial concentration (1.40 mg L^{-1}) with high concentration coexistence ions. When comparing to the two main coexistence ions—Al and Ca—the separation factors were SF(Ge/Al) = 42.57 and SF(Ge/Ca) = 39.93), respectively. After elution of the adsorbed Ge from TA-EPI-ORH, the extraction rate of Ge with low

initial concentration (1.40 mg L^{-1}) reached 85.17%, while the extraction rates of Al and Ca were only 1.02% and 1.18%, respectively. The results of this study provide an important theoretical basis and application reference for the efficient and environmentally friendly extraction of Ge from agricultural waste. These findings not only help to promote the sustainable use of rare metal resources, but also provide new ideas for the resource utilization of agricultural waste.

Author Contributions: Conceptualization, Q.W., W.Z., S.D., Z.S., X.S. and Y.W.; Data curation, W.Z.; Funding acquisition, Z.S.; Investigation, Q.W.; Methodology, Q.W., W.Z. and Z.S.; Project administration, Z.S.; Resources, Q.W. and S.D.; Supervision, Z.S.; Writing—original draft, W.Z.; Writing—review and editing, Q.W., W.Z., C.N. and C.W.K.C. All authors have read and agreed to the published version of the manuscript.

Funding: This work was supported by the NSFC Joint Program (No.U21A20320) and AI-Enhanced Research Program of Shanghai Municipal Education Commission (SMEC-AI-DHUZ-07).

Data Availability Statement: The raw data supporting the conclusions of this article will be made available by the authors on request.

Conflicts of Interest: The authors declare no conflict of interest.

References

1. Rafiee, P.; Ghassa, S.; Moosakazemi, F.; Khosravi, R.; Siavoshi, H. Recovery of a critical metal from electronic wastes: Germanium extraction with organic acid. *J. Clean. Prod.* **2021**, *315*, 128223. [CrossRef]
2. Tan, Z.D.; Jin, X.; Zhen, Y.; Wei, C.; Li, X.B.; Deng, Z.G.; Li, M.T. Recovery of indium and germanium from In-Ge residue leaching solution using solvent extraction and tannin precipitation. *Sep. Purif. Technol.* **2023**, *323*, 124416. [CrossRef]
3. Moskalyk, R.R. Review of germanium processing worldwide. *Miner. Eng.* **2004**, *17*, 393–402. [CrossRef]
4. Frenzel, M.; Ketris, M.P.; Gutzmer, J. On the geological availability of germanium. *Miner. Depos.* **2014**, *49*, 471–486. [CrossRef]
5. Arroyo, F.; Fernández-Pereira, C. Hydrometallurgical recovery of germanium from coal gasification fly ash. solvent extraction method. *Ind. Eng. Chem. Res.* **2008**, *47*, 3186–3191. [CrossRef]
6. Huang, Y.F.; Wang, M.M.; Liu, B.B.; Su, S.P.; Sun, H.; Yang, S.Z.; Han, G.H. The extraction and separation of scarce critical metals: A review of gallium, Indium and germanium extraction and separation from solid wastes. *Separations* **2024**, *11*, 91. [CrossRef]
7. Nguyen, T.H.; Lee, M.S. A review on germanium resources and its extraction by hydrometallurgical method. *Miner. Process. Extr. Metall. Rev.* **2020**, *42*, 406–426. [CrossRef]
8. Hong, Y.; Di, H.K.; Li, S.W.; Yang, K.; Zhang, L.B. Mechanism of extracting germanium from Ge-Containing solution with tannins. *Metals* **2023**, *13*, 774. [CrossRef]
9. Drzazga, M.; Palmowski, A.; Benke, G.; Ciszewski, M.; Leszczynska-Sejda, K. Recovery of germanium and indium from leaching solution of germanium dross using solvent extraction with TOA, TBP and D2EHPA. *Hydrometallurgy* **2021**, *202*, 105605. [CrossRef]
10. Kamran Haghighi, H.; Irannajad, M.; Fortuny, A.; Sastre, A.M. Recovery of germanium from leach solutions of fly ash using solvent extraction with various extractants. *Hydrometallurgy* **2018**, *175*, 164–169. [CrossRef]
11. Liu, F.P.; Liu, Z.H.; Li, Y.H.; Wilson, B.P.; Liu, Z.Y.; Zeng, L.; Lundström, M. Recovery and separation of gallium(III) and germanium(IV) from zinc refinery residues: Part II: Solvent extraction. *Hydrometallurgy* **2017**, *171*, 149–156. [CrossRef]
12. Wang, P.C.; Liu, Z.H.; Zhang, T.; Liu, Z.Y.; Zhu, D.Q.; Jiang, T. Extraction mechanism of germanium in sulfate solutions using a tertiary amine (N235)-based solvent extraction system. *Sep. Purif. Technol.* **2023**, *311*, 123305. [CrossRef]
13. Hernández-Expósito, A.; Chimenos, J.M.; Fernández, A.I.; Font, O.; Querol, X.; Coca, P.; García Peña, F. Ion flotation of germanium from fly ash aqueous leachates. *Chem. Eng. J.* **2006**, *118*, 69–75. [CrossRef]
14. Cote, G.; Bauer, D. liquid–liquid extraction of germanium with oxine derivatives. *Hydrometallurgy* **1980**, *5*, 149–160. [CrossRef]
15. De Schepper, A. liquid–liquid extraction of germanium by LIX 63. *Hydrometallurgy* **1976**, *1*, 291–298. [CrossRef]
16. Tao, J.; Tao, Z.; Liu, Z.H. Review on resources and recycling of germanium, with special focus on characteristics, mechanism and challenges of solvent extraction. *J. Clean. Prod.* **2021**, *294*, 126217. [CrossRef]
17. Ahmad, K.; Shah, I.A.; Ali, S.; Khan, M.T.; Qureshi, M.B.A.; Shah, S.H.A.; Ali, A.; Rashid, W.; Gul, H.N. Synthesis and evaluation of Ca-doped ferrihydrite as a novel adsorbent for the efficient removal of fluoride. *Environ. Sci. Pollut. Res.* **2022**, *29*, 6375–6388. [CrossRef]

18. Patel, M.; Karamalidis, A.K. Catechol-Functionalized chitosan synthesis and selective extraction of germanium (IV) from acidic solutions. *Ind. Eng. Chem. Res.* **2023**, *62*, 2892–2903. [CrossRef]
19. Cui, W.; Wang, S.; Peng, J.; Zhang, L.; Zhang, G. Catechol-functionalized nanosilica for adsorption of germanium ions from aqueous media. *J. Sol-Gel Sci. Technol.* **2015**, *77*, 666–674. [CrossRef]
20. Arrambide Cruz, C.; Marie, S.; Arrachart, G.; Pellet-Rostaing, S. Selective extraction and separation of germanium by catechol based resins. *Sep. Purif. Technol.* **2018**, *193*, 214–219. [CrossRef]
21. Nozoe, A.; Abe, M.; Ohto, K.; Kawakita, H. Germanium recovery using polyphenol microspheres prepared by horseradish peroxidase reaction. *J. Chem. Technol. Biotechnol.* **2011**, *86*, 1374–1378. [CrossRef]
22. Nozoe, A.; Ohto, K.; Kawakita, H. Germanium recovery using catechol complexation and permeation through an anion-exchange membrane. *Sep. Sci. Technol.* **2012**, *47*, 62–65. [CrossRef]
23. Virolainen, S.; Heinonen, J.I.; Paatero, E. Selective recovery of germanium with N-methylglucamine functional resin from sulfate solutions. *Sep. Purif. Technol.* **2013**, *104*, 193–199. [CrossRef]
24. Yasuda, S.; Kawazu, K. Separation of germanium from ethylene glycol distillates by N-methylglucamine resin. *Sep. Sci. Technol.* **1991**, *26*, 1273–1277. [CrossRef]
25. Khan, A.S.; Chow, A. X-ray fluorescence spectrometric determination of germanium after extraction with polyurethane foam. *Anal. Chim. Acta* **1990**, *238*, 423–426. [CrossRef]
26. Marco-Lozar, J.P.; Cazorla-Amorós, D.; Linares-Solano, A. A new strategy for germanium adsorption on activated carbon by complex formation. *Carbon* **2007**, *45*, 2519–2528. [CrossRef]
27. Zhang, L.; Li, H.; Liu, X.; Kang, P. Sorption behavior of germanium(IV) on titanium dioxide nanoparticles. *Russ. J. Inorg. Chem.* **2012**, *57*, 622–628. [CrossRef]
28. Wu, X.Q.; Yuan, M.Y.; Guo, X.J.; Zhang, L. Fast coadsorption and selective separation of gallium(III) and germanium(IV) from aqueous solutions by 3D hierarchical porous hoya-like α-FeOOH. *ACS Sustain. Chem. Eng.* **2019**, *7*, 15939–15947. [CrossRef]
29. Geromel-Costa, C.G.A.; Corbi, J.J.; Gorni, G.R.; Colombo, V.; Correa, R.C.; Fiamingo, A.; Campana-Filho, S.P. Adsorption of metals by crosslinked chitosan beads in sugarcane contaminated streams. *Biomass Bioenergy* **2018**, *119*, 128–134. [CrossRef]
30. Li, Y.; Tsend, N.; Li, T.; Liu, H.; Yang, R.; Gai, X.; Wang, H.; Shan, S. Microwave assisted hydrothermal preparation of rice straw hydrochars for adsorption of organics and heavy metals. *Bioresour. Technol.* **2019**, *273*, 136–143. [CrossRef]
31. Ye, H.; Zhu, Q.; Du, D. Adsorptive removal of Cd(II) from aqueous solution using natural and modified rice husk. *Bioresour. Technol.* **2010**, *101*, 5175–5179. [CrossRef] [PubMed]
32. Bhatnagar, A.; Sillanpää, M. Utilization of agro-industrial and municipal waste materials as potential adsorbents for water treatment—A review. *Chem. Eng. J.* **2010**, *157*, 277–296. [CrossRef]
33. Xiong, Y.; Cui, X.; Wang, D.; Wang, Y.; Lou, Z.; Shan, W.; Fan, Y. Diethanolamine functionalized rice husk for highly efficient recovery of gallium(III) from solution and a mechanism study. *Mater. Sci. Eng. C* **2019**, *99*, 1115–1122. [CrossRef]
34. O'Connell, D.W.; Birkinshaw, C.; O'Dwyer, T.F. Heavy metal adsorbents prepared from the modification of cellulose: A review. *Bioresour. Technol.* **2008**, *99*, 6709–6724. [CrossRef]
35. Zheng, L.; Zhu, C.; Dang, Z.; Zhang, H.; Yi, X.; Liu, C. Preparation of cellulose derived from corn stalk and its application for cadmium ion adsorption from aqueous solution. *Carbohydr. Polym.* **2012**, *90*, 1008–1015. [CrossRef]
36. Zhang, Y.Y.; Zhu, L.; Wang, Y.; Lou, Z.N.; Shan, W.J.; Xiong, Y.; Fan, Y. Preparation of a biomass adsorbent for gallium(III) based on corn stalk modified by iminodiacetic acid. *J. Taiwan Inst. Chem. Eng.* **2018**, *91*, 291–298. [CrossRef]
37. Du, J.F.; Zhang, M.M.; Dong, Z.; Yang, X.; Zhao, L. Facile fabrication of tannic acid functionalized microcrystalline cellulose for selective recovery of Ga(III) and In(III) from potential leaching solution. *Sep. Purif. Technol.* **2022**, *286*, 120442. [CrossRef]
38. Hossain, M.F.; Akther, N.; Lu, J.; Duan, C.; Khan, M.T.; Munyaneza, J.; Zhou, Y. Highly effective and reusable cellulose-based amphoteric adsorbent for dye removal from single and binary system. *Int. J. Environ. Sci. Technol.* **2025**. [CrossRef]
39. Wang, Y.C.; Jiang, X.; Zhang, C.; Jing, X.L.; Liu, Y.H. Synthesis of epoxide functionalized hyperbranched polyurethane and its blending with benzoxazine: Cure kinetics and thermal properties. *Polym. Bull.* **2017**, *74*, 4209–4222. [CrossRef]
40. Patel, M.; Karamalidis, A.K. Germanium: A review of its US demand, uses, resources, chemistry, and separation technologies. *Sep. Purif. Technol.* **2021**, *275*, 118981. [CrossRef]
41. Cheng, Y.X.; He, P.; Dong, F.Q.; Nie, X.Q.; Ding, C.C.; Wang, S.; Zhang, Y.; Liu, H.H.; Zhou, S.P. Polyamine and amidoxime groups modified bifunctional polyacrylonitrile-based ion exchange fibers for highly efficient extraction of U(VI) from real uranium mine water. *Chem. Eng. J.* **2019**, *367*, 198–207. [CrossRef]
42. Tran, H.N.; Lima, E.C.; Juang, R.-S.; Bollinger, J.-C.; Chao, H.-P. Thermodynamic parameters of liquid–phase adsorption process calculated from different equilibrium constants related to adsorption isotherms: A comparison study. *J. Environ. Chem. Eng.* **2021**, *9*, 106674. [CrossRef]

43. Park, H.J.; Tavlarides, L.L. Germanium(IV) adsorption from aqueous solution using a Kelex-100 functional adsorbent. *Ind. Eng. Chem. Res.* **2009**, *48*, 4014–4021. [CrossRef]
44. Raj, P.; Patel, M.; Karamalidis, A.K. Chemically modified polymeric resins with catechol derivatives for adsorption, separation and recovery of gallium from acidic solutions. *J. Environ. Chem. Eng.* **2023**, *11*, 110790. [CrossRef]

Disclaimer/Publisher's Note: The statements, opinions and data contained in all publications are solely those of the individual author(s) and contributor(s) and not of MDPI and/or the editor(s). MDPI and/or the editor(s) disclaim responsibility for any injury to people or property resulting from any ideas, methods, instructions or products referred to in the content.